Graphene-based bipolar spin diode and spin transistor: Rectification and amplification of spin-polarized current

Minggang Zeng,[1,2] Lei Shen (沈雷),[1,*] Miao Zhou (周苗),[1] Chun Zhang,[1,3] and Yuanping Feng[1,†]
[1]*Department of Physics, 2 Science Drive 3, National University of Singapore, Singapore 117542, Singapore*
[2]*NanoCore, 5A Engineering Drive 4, National University of Singapore, Singapore 117576, Singapore*
[3]*Department of Chemistry, 3 Science Drive 3, National University of Singapore, Singapore 117543, Singapore*
(Received 8 January 2011; published 14 March 2011)

Using nonequilibrium Green's function method combined with density functional theory we report bipolar spin diode behavior in zigzag graphene nanoribbons (ZGNRs). Nearly ±100% spin-polarized current can be generated and tuned by a source-drain voltage and/or magnetic configurations in these two-terminal bipolar spin diodes. This unique transport property is attributed to the intrinsic transmission selection rule of the wave function of spin subbands near the Fermi level in ZGNRs. Moreover, the bias voltage and magnetic configurations of the two-terminal ZGNR-based spin diodes provide a rich variety of ways to control the spin current, which can be used to design three-terminal spin transistors. These ZGNRs-based components make possible the manipulation of spin-polarized current such as rectification and amplification for carbon-based spintronics.

DOI: 10.1103/PhysRevB.83.115427 PACS number(s): 73.22.Pr, 71.15.Mb, 85.75.Hh

I. INTRODUCTION

Spintronics, a new type of electronics that exploits the spin degree of freedom of an electron in addition to its charge, offers one of the most promising solutions for future high operating speed and energy-saving electronic devices.[1] The major challenge of spintronics is the difficulty in generating, controlling, and detecting spin-polarized current. This situation is expected to change with successful development of spintronics devices based on graphene, an atomically thin carbon sheet.[2,3] Since graphene was discovered experimentally in 2004,[2] its applications in future electronics and spintronics have been a major research focus and to date a number of major breakthroughs have been made. Recently, spin injection in graphene has been demonstrated using a cobalt electrode at room temperature.[4] Maassen *et al*. theoretically predicted that the spin injection efficiencies from a ferromagnetic electrode into graphene can reach 60%–80%. More recently, Han *et al*. proposed that the efficiency of spin injection from a ferromagnetic electrode into graphene can be enhanced by a tunneling barrier.[5] Some graphene-based tunneling field effect transistors (FETs) were proposed by Guo *et al*.[6,7] Besides spin injection, spin detection in graphene has also been realized using a nonlocal measurement method in which spin-up and spin-down currents can be distinguished and measured independently.[4] Moreover, graphene nanoribbon is known to have long spin diffusion length, spin relaxation time, and electron spin coherence time.[8–10] GNRs can be used as spin generation materials such as electrodes as well as spin injection materials.[11–13] All of these show that graphene hold the promise of spintronics.[8,14] A variety of graphene-based spintronics devices have been proposed.[11,15–19] For example, a graphene nanoribbon-based giant magnetoresistance (GMR) device has been proposed theoretically and realized experimentally which is useful for information storage.[15,16,20] Wang *et al*. also experimentally observed large MR in graphene-based devices.[17] However, most of these studies have been on individual components and focused mainly on devices for information storage. There has not been any implementation for the full range of spintronic devices. Developments of multifunctional graphene-based spintronics components such as devices that offer effective manipulation of spin-polarized current are crucial for a complete realization of spintronics.

In this article we explore possible control of spin-polarized current in zigzag graphene nanoribbons (ZGNRs) and discuss possible design of ZGNR-based devices. We demonstrate that spin polarization of a current in a ZGNR-based two-terminal device can be tuned by a source-drain voltage and the device functions as a bipolar spin diode. This is possible because of a symmetry selection rule. As we know, spin-polarized current is normally produced using "half-metallic" materials such as graphene nanoribbons under transverse electric fields,[21,22] organometallic sandwich molecular wires,[23] and group III/V semiconductors.[24,25] Generation of spin-polarized current using an intrinsic symmetry selection rule proposed here is a totally different concept. We also propose the use of magnetic configurations [±1,0], that is, one electrode is magnetized while the other is nonmagnetic in the design, in addition to the conventional parallel [1,1]/anti-parallel [1,−1] magnetic configurations of GMR devices. The biggest advantage of the [±1,0] magnetic configurations is that it allows reduction of design complexity since only one electrode needs to be magnetized. It also avoids direct magnetic interaction between the two magnetic electrodes if the central part of nanodevices is very small. Finally, no minimum working voltage is needed due to the zero threshold voltage in the sub-10-nm GNR-based devices in the [±1,0] magnetic configurations. These novelties of GNR-based spintronic components offer flexibility in manipulating spin current and allow the designs of spintronic devices which provide the essential components for a future spintronic integrated circuit.

II. METHODOLOGY

The spin-dependent quantum transport calculations were carried out within the framework of density functional theory (DFT) combined with nonequilibrium Green's function

 ©2011 American Physical Society

(NEGF) method as implemented in the Atomistix ToolKit software package.[26,27] The local spin density approximation (LSDA) proposed by Perdew and Zunger was adopted for exchange and correlation functional,[28] and the single-ζ basis set was used for electron wave function which has been proved to well describe the π-conjugated bond system and the transport calculation including transmission and current-voltage characteristics.[15] A cutoff energy of 150 Ry and a Monkhorst-Pack k mesh of $1 \times 1 \times 100$ yielded a good balance between computational time and accuracy in the results. The spin-polarized current through the system was calculated from

$$I^{\uparrow(\downarrow)}(V_b) = \frac{e}{h}\int_{-\infty}^{\infty}\{T^{\uparrow(\downarrow)}(\varepsilon, V_b)[f_L(\varepsilon, V_b) - f_R(\varepsilon, V_b)]\}d\varepsilon, \tag{1}$$

where $f_{L(R)}(\varepsilon, V_b) = n_F(\varepsilon - \mu_{L(R)})$. n_F and $\mu_{L(R)}$ are the Fermi function and the electrochemical potentials of the left (right) lead, respectively. $T^{\uparrow(\downarrow)}(\varepsilon, V_b)$ is the spin-resolved transmission defined as

$$T^{\uparrow(\downarrow)}(\varepsilon, V_b) = Tr\left[\mathrm{Im}\left\{\Sigma^r_{L\uparrow(\downarrow)}(\varepsilon, V_b)\right\}G^r_{\uparrow(\downarrow)}(\varepsilon, V_b) \times \mathrm{Im}\left\{\Sigma^r_{R\uparrow(\downarrow)}(\varepsilon, V_b)\right\}G^a_{\uparrow(\downarrow)}(\varepsilon, V_b)\right], \tag{2}$$

where $\sum^r_{L/R}$ is the retarded self-energy matrix which takes into account the left and right leads. $G^r(G^a)$ is the retarded (advanced) Green's function matrix. Contour integration was carried out in the imaginary plane to obtain the density matrix from the Green's function. We used 30 contour points with a lower energy bound of 3 Ry in the contour diagram in the case of zero bias and additional contour points spaced at 0.02 eV along the real energy axis in the case of nonzero bias. The NEGF-DFT self-consistency was controlled by a numerical tolerance of 10^{-5} eV. The electron temperature is set to 300 K in the transport calculation. In all the calculations, dangling bonds at the edges of GNRs are saturated with pseudohydrogen atoms. A 15 Å vacuum slab was used to eliminate interaction between ZGNRs in neighboring cells.

III. RESULTS AND DISCUSSION

A. Spin diode

Structures of all graphene nanoribbons being studied were fully optimized and the C-C and C-H bond distances in the optimized graphene nanoribbons are 1.42 and 1.10 Å, respectively. Figure 1 shows the schematic configuration of a two-terminal ZGNR-based spin device. Magnetization of each ZGNR electrode can be controlled by an external magnetic field[15–17] and can be set to 1 (magnetization along the $+y$ direction shown in Fig. 1), 0 (nonmagnetic), or -1 (magnetization along the $-y$ direction). We denote the magnetization of the left (right) electrode by M_L (M_R) (=1,0, or -1). Current flows along z ($-z$) direction is defined as the $+$ ($-$) direction, corresponding to a positive (negative) applied bias voltage. A ZGNR with N zigzag chains is denoted by N-ZGNR.[29] We focus on the case in which N is even since previous study has concluded that only ZGNR with an even number of zigzag chain shows the transmission selection rule, which is related to the symmetry of ZGNRs.[30]

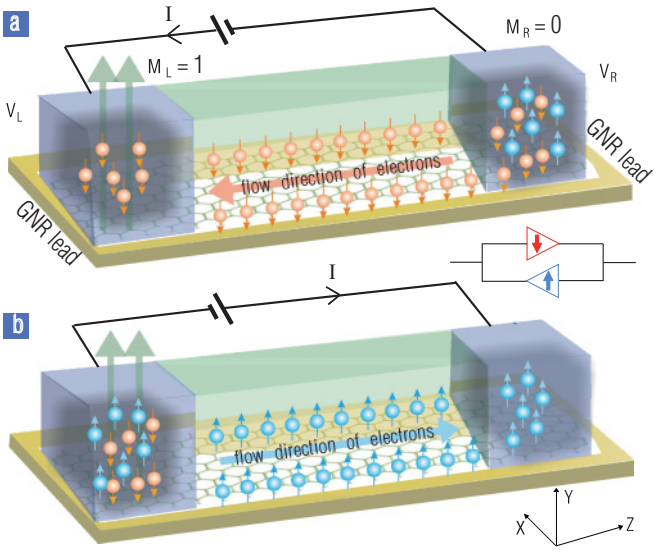

FIG. 1. (Color online) Schematic diagram of ZGNRs-based *bipolar* spin diodes. An external magnetic field is used to magnetize one or both GNR leads. M_L and M_R represent the magnetization of the left and right leads under the magnetic field, respectively. The value of M_L and M_R can be 1, 0, or -1, corresponding to magnetization along the $+y$ direction, nonmagnetic lead, and magnetization along the $-y$ direction, respectively. (a) Under a positive bias only spin-down electrons transport through devices. Note that the flow direction of electrons is from right to left leads while the flow direction of current is from left to right leads. (b) Under a negative bias only spin-up electrons are allowed to transport from left to right leads. It behaves as a bias-controlled bipolar spin diode device. The circuit diagram of this bias-controlled bipolar spin diode is shown in the inset.

Following the conventional approach used in GMR spintronic devices, we consider first the spin-polarized current in the two-terminal device under the magnetic configurations $[M_L, M_R] = [1,1]$ and $[1,-1]$, respectively. Figure 2 shows the transmission spectra and I-V curves under the magnetic configurations of $[1,1]$ and $[1,-1]$. The up and down triangles shown by the intersecting solid straight lines are referred to the bias window and only transmission within the bias window contributes to the current. Therefore, the properties of I-V curves can be understood based on the transmission spectra. For example, in the spin-up state of $[1,1]$ configuration [see Fig. 2(a)] the area within the bias window increases linearly under a low positive or negative bias (less than 0.4 V) resulting in a linear I-V curve [region I in Fig. 2(b)]. Once the bias voltage reaches 0.4 V, the rate of increase of the area of transmission within the bias window becomes a constant, which results in the saturation of the I-V current [region II in Fig. 2(b)]. The spin-down state of the $[1,1]$ configuration shows similar property [as shown in Figs. 2(c) and 2(d)]. The transport and electronic properties of the $[1,1]$ system are in agreement with those of Refs. 15 and 20. Interestingly, in the $[1,-1]$ configuration the spin transport property under a negative bias is completely opposite of that under a positive bias. Figures 2(e) and 2(g) show the transmission spectra of magnetic configuration of $[1,-1]$. As can be seen, the spin-up transmission within the bias window is always zero under a positive bias. Thus the spin-up current is always suppressed

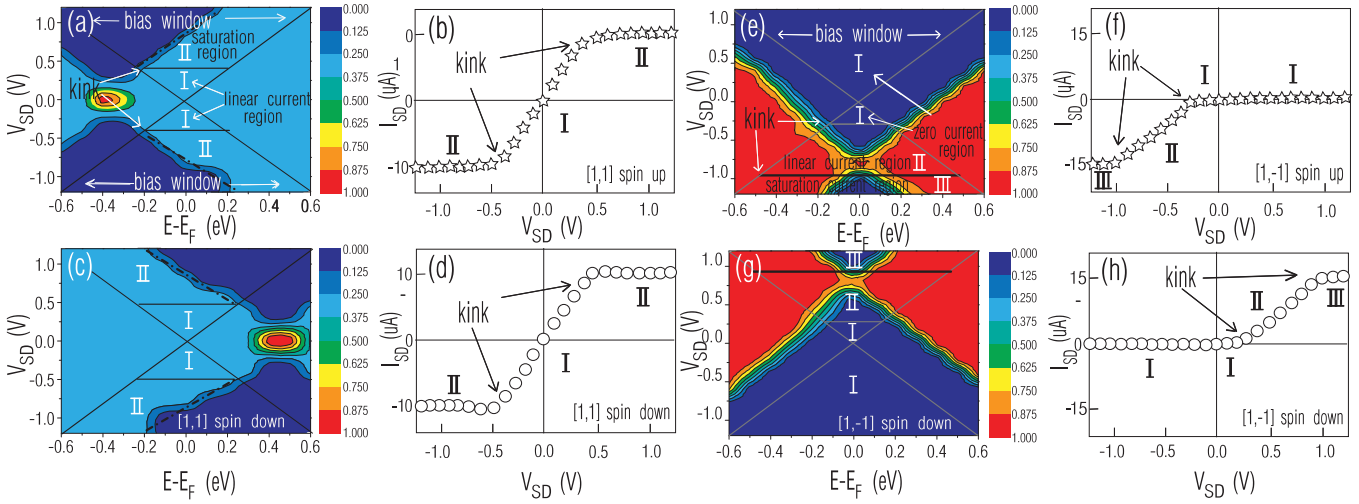

FIG. 2. (Color online) Spin-dependent transmission spectrum as a function of electron energy E, bias V_{SD}, and I-V curve, respectively, for different spins and under various magnetic configurations of the electrodes. (a) and (b) Spin-up state in the magnetic configuration [1,1]. (c) and (d) Spin-down state in [1,1]. (e) and (f) Spin-up state in [1,−1]. (g) and (h) Spin-down state in [1,−1]. The up and down triangles shown by the intersecting solid straight lines are the bias windows which sets boundaries for transmission that contributes to the current at a given bias voltage. The Fermi energy is set to zero.

under the positive bias [region I in Fig. 2(f)]. Under a negative bias the variation of the current with the bias voltage goes through three different stages. At a small bias (less than 0.25 V) the transmission is zero, resulting in a suppressed current [region I in Fig. 2(f)]. At an intermediate bias voltage (0.25 to 0.95 V) the rate of increase of the transmission area with the bias voltage is linear, leading to a linear I-V curve [region II in Fig. 2(f)]. Once the bias voltage is above 0.95 V the rate of increase of the transmission area within the bias window becomes a constant, which results in the saturation of the current through the device [region III in Fig. 2(f)]. In a brief summary, under a positive bias only the spin-down current is allowed to pass through the device, while under a negative bias only the spin-up current is possible. In other words, the spin polarization of the current can be selectively generated by the source-drain voltage in the single device. A device with such properties is referred to a bipolar spin diode[31] or a dual spin filter[32] because its operation involves both spin-up and spin-down polarized currents. It is different from the traditional bipolar devices based on electron and hole carrier types or polarized and unpolarized states in graphene-based memory devices.[33]

We also considered the dependence of the transport property on the width of the ZGNRs. In Fig. 3 we show the transmission

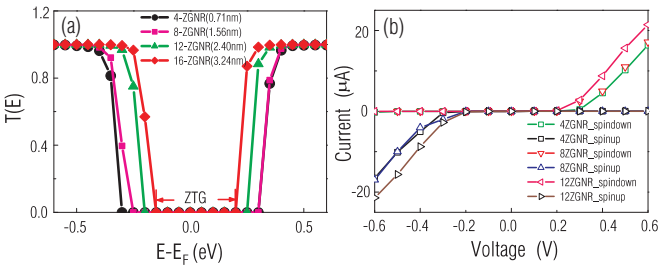

FIG. 3. (Color online) Ribbon width dependence of transmission spectrum and I-V curve showing decrease of both the zero transmission gap (ZTG) and the threshold voltage with the increase of ribbon width.

of unpolarized N-ZGNRs ($N = 4, 8, 12, 16$) and the I-V curves of spin-polarized N-ZGNRs ($N = 4, 8, 12$). As can be seen, the zero transmission gap (ZTG) and the threshold voltage decrease with the increase of ribbon width. Therefore, when the ribbon is sufficiently wide, the ZTG and threshold voltage would diminish and the devices would show a metallic behavior under a negative bias but an insulating property under a positive bias for the spin-up current. The behavior of the spin-down current is exactly the opposite, that is, insulating under a negative bias and metallic under a positive bias.

Besides the traditional parallel [1,1] and antiparallel [1,−1] magnetic configurations of the electrodes, we considered here also spin-dependent transport in the magnetic configurations [1,0] and [−1,0]. The "0" represents the nonmagnetic state which is possible considering the limited spin correlation length due to the unstable one-dimensional spin ordering and the width and temperature-dependent ground state in ZGNRs.[8,15] One clear advantage of the [±1,0] magnetic configurations, compared to [1,±1], is that it allows reduction of design complexity since only one electrode needs to be magnetized. Another advantage would be that it avoids direct magnetic interaction between the two magnetic electrodes if the central part of nanodevices is small. The calculated spin-dependent transmission spectra as a function of electron energy E, bias V_{SD}, and the I-V curves are shown in Fig. 4. The bipolar spin diode behavior can be clearly seen in these configurations similar to those in the [1,−1] configuration [Fig. 2(a)] with only exceptions of a small leakage current and a zero threshold voltage in the [1,0] and [−1,0] configurations which indicate that no minimum working voltage is required to operate such devices. The calculated I-V curves in the [1,0] and [−1,0] configurations suggest that the spin-up or spin-down conducting channel can be switched by either the bias direction or the magnetization of the ZGNR electrode (as schematically illustrated in Fig. 1). This selective spin current through the device is attributed to the orbital symmetry of spin

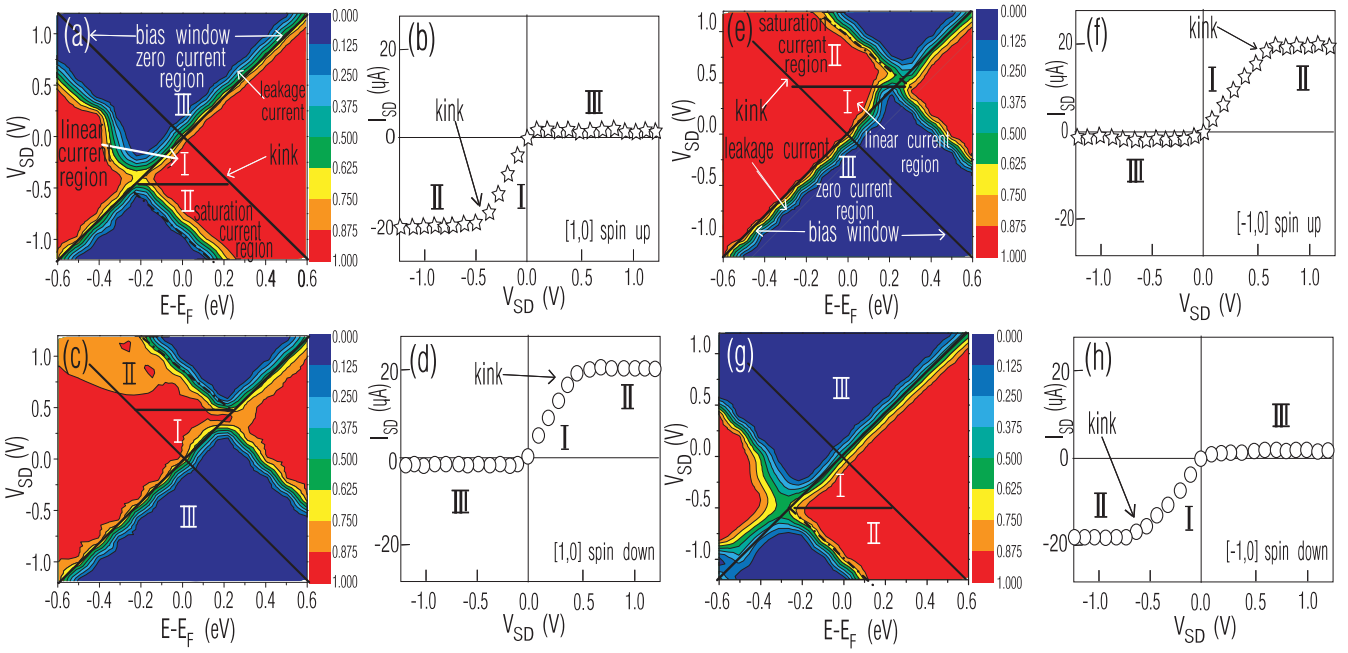

FIG. 4. (Color online) Spin-dependent transmission spectrum as a function of electron energy E, bias V_{SD}, and I-V curve, respectively, for various spin states and magnetic configurations of the electrodes. (a) and (b) Spin-up state in magnetic configuration [1,0]. (c) and (d) Spin-down state in [1,0]. (e) and (f) Spin-up state in [−1,0]. (g) and (h) Spin-down state in [−1,0]. The up and down triangles shown by the intersecting solid straight lines are the bias windows which sets boundaries for transmission that contributes to the current at a given bias voltage. The Fermi energy is set to zero.

subbands[30] and can be understood from the band structure of the left and right electrodes shown in Figs. 5(a) and 5(b) for the [1,0] configuration. The π and π^* subbands in the nonmagnetic right electrode are spin degenerate and cross the Fermi level, while those in the magnetic left electrode are split. At zero bias transmission is forbidden in certain energy ranges [such as those indicated by arrows in Fig. 5(a)] due to mismatch of symmetries of electron wave functions of the π^* and π subbands. As shown in Figs. 5(c) and 5(d) the π^* subbands have the σ symmetry, while the π subbands show C_2 symmetry. However, shifts of energy bands induced by a small positive bias open the spin-down channel while they keep the spin-up channel closed due to the symmetry match of spin-down subbands and mismatch of the spin-up subbands in the left and right electrodes. The effect of a negative bias is similar except that the spin-up channel is selected while the spin-down channel is blocked. Therefore, the transmission selection rule of the spin subbands near the Fermi level is attributed to symmetry allowed transmission of one spin channel ($\sigma \leftrightarrow \sigma$) and symmetry mismatch for the other spin channel ($\sigma \leftrightarrow \sigma^*$) between the two electrodes.

B. Spin current amplifier

The above results indicate that all three magnetic configurations [1,−1], [1,0], and [−1,0] of the two-terminal device exhibit spin diode behavior and the conducting spin channel can be selected by setting proper bias direction (+ or −) and/or magnetic configuration (1, 0, or −1) of the left and right electrodes. This flexible control over spin current makes it possible to use the two-terminal device as a basic component for building multifunctional spintronic devices such as spin transistors. The first device we propose here is a spin transistor for current amplification. Two designs of the transistor, one for spin-up current and one for spin-down current, are shown in Figs. 6(a) and 6(b), respectively. A sideview of the device is shown in Fig. 6(c). Each transistor consists of three terminals, an emitter, a collector, and a base. The only difference between the two designs is the magnetic configurations of the electrodes which are indicated in Fig. 6. The emitter is grounded and the collector voltage (V_C) is fixed to a positive value, while the voltage of the base (V_B) can be varied which controls the flow and polarization of the current. The polarity of the spin transistor is determined by the magnetic configuration between the emitter and the collector. In Fig. 6(a) the magnetic configuration between the emitter and the base is [1,0] and the bias voltage is negative. Based on the I-V property shown in Figs. 4(b) and 4(d) the current I_E contains only spin-up electrons. Between the collector and the base the magnetic configuration is [−1,0] and the bias voltage is positive as long as $V_B < V_C$, according to the I-V curve shown in Figs. 4(f) and 4(h) only the spin-up electrons are allowed to flow from the base to the collector. Similarly, the design shown in Fig. 6(b) allows only spin-down electrons to pass through the device. The equivalent circuit diagrams are shown in Figs. 6(d) and 6(e), respectively. According to the I-V curve shown in Fig. 4, $I = GV$ under a small bias (−0.4–0.4 V), where G is the conductance. The current gain is defined as

$$\left|\frac{I_C}{I_B}\right| = \left|\frac{I_C}{I_E - I_C}\right| = \left|\frac{G(V_C - V_B)}{G(V_B - V_E) - G(V_C - V_B)}\right| = \left|\frac{1 - V_B/V_C}{2V_B/V_C - 1}\right|. \quad (3)$$

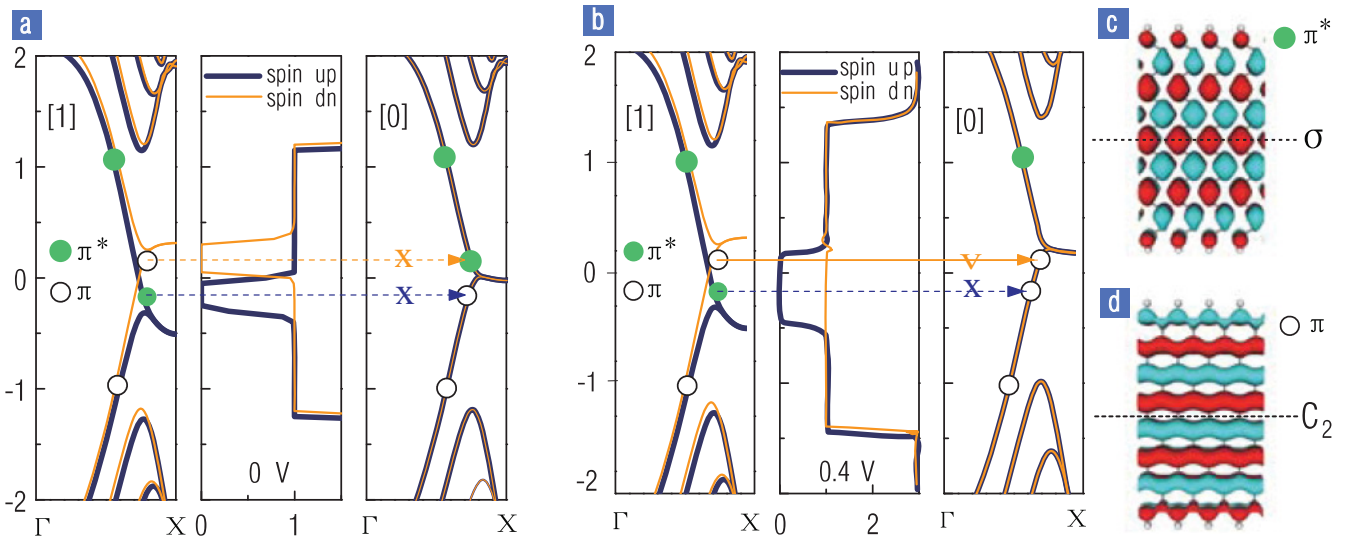

FIG. 5. (Color online) (a) Band structure of the magnetized left lead (left panel), transmission curve (middle panel), and band structure of the nonmagnetic right lead (right panel) of the device shown in Fig. 1 at zero bias. The spin-up bands are shown in blue while the spin-down bands are given in orange. The dashed (solid) line with an arrow illustrates a forbidden (allowed) hopping of electrons from the left lead to the right lead due to the symmetry mismatching (matching) of the π and π^* subbands. (b) The same information as (a) but for a positive bias (+0.4 V). The transmission gap for spin-down is reduced but that for spin-up is increased compared to that in Figs. 4(g) and 4(e) which opens spin-down channel and suppresses spin-up channel as in Figs. 4(h) and 4(f). (c) and (d) Isosurface plots of the Γ-point wave functions of π^* and π subbands for 8-ZGNR. Red and blue indicate opposite signs of the wave function.

The current gain (I_C/I_B) based on Eq. (3) is shown as a function of V_B/V_C in Fig. 6(f). The current gain is equal to 1 when $V_B = 0$ and goes to zero when $V_B = V_C$, but it increases dramatically near $V_B/V_C = 1/2$, which suggests a high-performance ZGNR-based three-terminal spin transistor. The amplification of spin-polarized current is also useful for detection of spin-polarized current.

C. Spin voltage amplifier

Transistors operating as voltage amplifiers can be designed similarly. In Figs. 6(g) and 6(h) we show a possible Johnson type of design.[34] Here the emitter and base are similar to those in the current amplifiers but the collector is replaced by a cobalt and graphene junction. The ferromagnetic cobalt

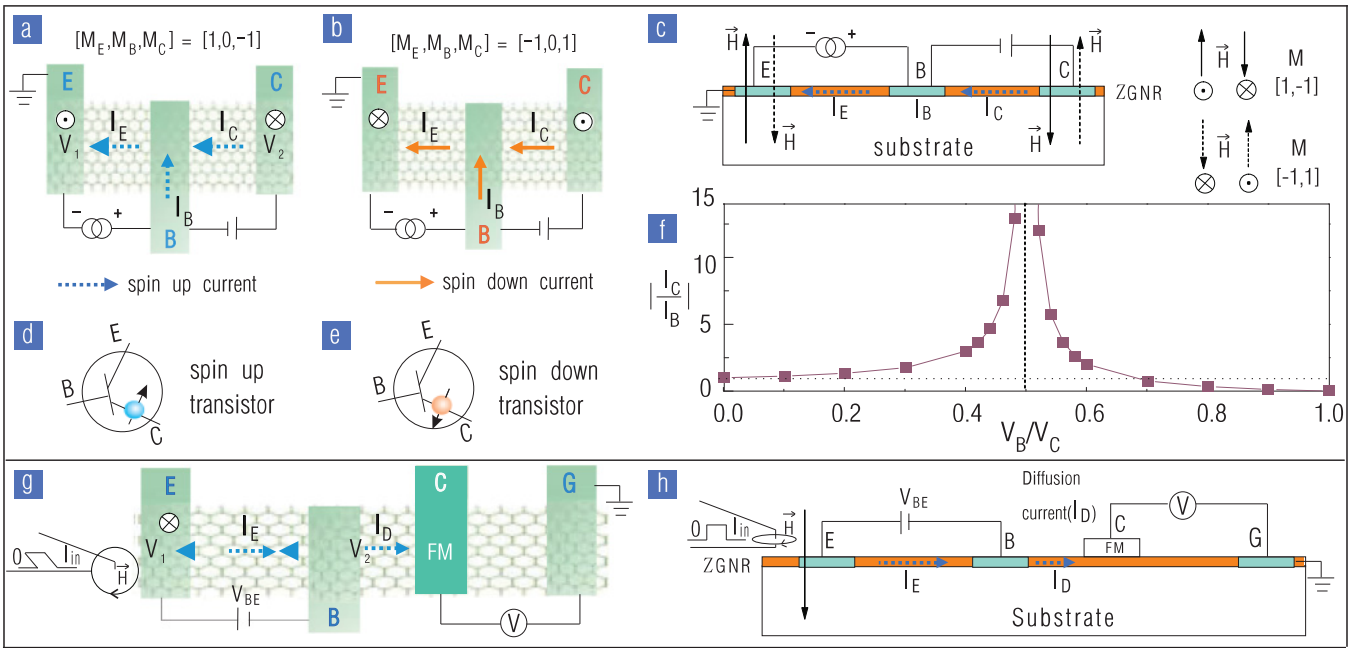

FIG. 6. (Color online) Schematic illustrations of ZGNR-based transistors with current and voltage amplification functions, respectively. (a)–(c) Top and sideviews of the current-amplifying three-terminal spin-up and spin-down transistors. (d) and (e) The circuit symbols of spin-up and spin-down transistors, respectively. (f) The current gain ($|I_C/I_B|$) as a function of V_B/V_C based on Eq. (3). (g) and (h) Top and side views of a Johnson-type transistor as a voltage amplifier.

electrode is used to detect the spin-polarized current (up or down). The spin-polarized current will flow from the emitter to the base under a bias voltage and then diffuses from the base to the collector (I_d), generating a voltage difference V_d across the cobalt and graphene junction which can be measured. At a fixed diffuse distance V_d is determined by the injected spin-polarized current at the base, which is linearly dependent on $V_{\rm BE}$. Therefore we can have $V_d = \alpha V_{\rm BE}$, where α is a constant. On the other hand, the magnetization of the emitter can be manipulated by placing a conducting wire with a current $I_{\rm in}$ next to it. Thus the voltage gain of this transistor is $\beta = V_d/V_{\rm in} = (\alpha V_{\rm BE})/(I_{\rm in}R_{\rm in})$. With proper choices of the parameters it is possible for the transistor to act as a voltage amplifier. Compared with the conventional spin transistors, ZGNR-based spin transistors possess several unique features. First, the injected current from the emitter to the base is completely spin polarized. Second, graphene is a much better spin transport medium because the spin diffusion length in graphene is much longer than that in metal. In addition, the spin polarization of the current can be simply tuned by switching either the magnetization of the emitter-ZGNR or the dc bias direction, providing adjustable bipolar spin transistors.

IV. SUMMARY

In summary, our first-principles studies on spin-dependent transport properties show that a bias-controlled bipolar spin diode behavior is an intrinsic property of biased ZGNRs which arises from the symmetry matching of wave functions of the two different subbands near the Fermi level. Spin polarization and direction of the current through the device can be controlled through either the source-drain voltage or magnetic configuration of the electrodes. Such freedom in controlling the spin-polarized current in ZGNR-based spin diodes allows us to theoretically design three-terminal spin transistors. These spin components can perform basic functions of spintronics devices such as rectification and amplification, and make it possible to manipulate spin-polarized current for the graphene-based nanospintronics.

ACKNOWLEDGMENT

This work is partially supported by the National Research Foundation (Singapore) Competitive Research Program (Grant No. NRF-G-CRP 2007-05).

*shenlei@nus.edu.sg
†phyfyp@nus.edu.sg

[1] S. A. Wolf, D. D. Awschalom, R. A. Buhrman, J. M. Daughton, S. von Molnár, M. L. Roukes, A. Y. Chtchelkanova, and D. M. Treger, Science **294**, 1488 (2001).
[2] K. S. Novoselov, A. K. Geim, S. V. Morozov, D. Jiang, Y. Zhang, S. V. Dubonos, I. V. Grigorieva, and A. A. Firsov, Science **306**, 666 (2004).
[3] K. S. Novoselov, A. K. Geim, S. V. Morozov, D. Jiang, M. I. Katsnelson, I. V. Grigorieva, S. V. Dubonos, and A. A. Firsov, Nature (London) **438**, 197 (2005).
[4] N. Tombros, C. Jozsa, M. Popinciuc, H. T. Jonkman, and B. J. van Wees, Nature (London) **448**, 571 (2007).
[5] W. Han, K. Pi, K. M. McCreary, Y. Li, J. J. I. Wong, A. G. Swartz, and R. K. Kawakami, Phys. Rev. Lett. **105**, 167202 (2010).
[6] J. C. P. Zhao and J. Guo, Nano Lett. **9**, 684 (2009).
[7] Y. Lu and J. Guo, Appl. Phys. Lett. **97**, 073105 (2010).
[8] O. V. Yazyev and M. I. Katsnelson, Phys. Rev. Lett. **100**, 047209 (2008).
[9] O. V. Yazyev, Nano Lett. **8**, 1011 (2008).
[10] G. Cantele, Y.-S. Lee, D. Ninno, and N. Marzari, Nano Lett. **9**, 3425 (2009).
[11] M. Koleini, M. Paulsson, and M. Brandbyge, Phys. Rev. Lett. **98**, 197202 (2007).
[12] M. G. Zeng, L. Shen, Y. Q. Cai, Z. D. Sha, and Y. P. Feng, Appl. Phys. Lett. **96**, 042104 (2010).
[13] L. Shen, M. G. Zeng, S.-W. Yang, C. Zhang, X. F. Wang, and Y. P. Feng, J. Am. Chem. Soc. **132**, 11481 (2010).
[14] A. H. Castro Neto and F. Guinea, Phys. Rev. Lett. **103**, 026804 (2009).
[15] W. Y. Kim and K. S. Kim, Nat. Nanotechnol. **3**, 408 (2008).
[16] J. W. Bai, X. Zhong, S. Jiang, Y. Huang, and X. F. Duan, Nat. Nanotechnol. **5**, 190 (2010).
[17] W. H. Wang, K. Pi, Y. Li, Y. F. Chiang, P. Wei, J. Shi, and R. K. Kawakami, Phys. Rev. B **77**, 020402 (2008).
[18] J. A. Furst, T. G. Pedersen, M. Brandbyge, and A.-P. Jauho, Phys. Rev. B **80**, 115117 (2009).
[19] C. Jozsa, M. Popinciuc, N. Tombros, H. T. Jonkman, and B. J. van Wees, Phys. Rev. Lett. **100**, 236603 (2008).
[20] Y.-T. Zhang, H. Jiang, Q.-F. Sun, and X. C. Xie, Phys. Rev. B **81**, 165404 (2010).
[21] Y.-W. Son, M. L. Cohen, and S. G. Louie, Nature (London) **444**, 347 (2006).
[22] J. Guo, D. Gunlycke, and C. T. White, Appl. Phys. Lett. **92**, 163109 (2008).
[23] L. Shen, S. W. Yang, M. F. Ng, V. Ligatchev, L. P. Zhou, and Y. P. Feng, J. Am. Chem. Soc. **130**, 13956 (2008).
[24] M. H. Wu, Z. H. Zhang, and X. C. Zeng, Appl. Phys. Lett. **97**, 093109 (2010).
[25] K. S. Yang, R. Q. Wu, L. Shen, Y. P. Feng, Y. Dai, and B. B. Huang, Phys. Rev. B **81**, 125211 (2010).
[26] M. Brandbyge, J. L. Mozos, P. Ordejon, J. Taylor, and K. Stokbro, Phys. Rev. B **65**, 165401 (2002).
[27] J. Taylor, H. Guo, and J. Wang, Phys. Rev. B **63**, 121104 (2001).
[28] J. P. Perdew and Y. Wang, Phys. Rev. B **45**, 13244 (1992).
[29] Y. W. Son, M. L. Cohen, and S. G. Louie, Phys. Rev. Lett. **97**, 216803 (2006).
[30] Z. Li, H. Qian, J. Wu, B.-L. Gu, and W. Duan, Phys. Rev. Lett. **100**, 206802 (2008).
[31] M. G. Zeng, L. Shen, M. Yang, C. Zhang, and Y. P. Feng, Appl. Phys. Lett. **98**, 053101 (2011).
[32] T. Ozaki, K. Nishio, H. M. Weng, and H. Kino, Phys. Rev. B **81**, 075422 (2010).
[33] D. Gunlycke, D. A. Areshkin, J. W. Li, J. W. Mintmire, and C. T. White, Nano Lett. **7**, 3608 (2007).
[34] P. R. Hammar and M. Johnson, Phys. Rev. Lett. **88**, 066806 (2002).